Achievable Rate Region and Optimality of Multi-hop Wireless 802.11-Scheduled Networks

Apoorva Jindal
Department of Electrical Engineering
University of Southern California
Los Angeles, CA 90089
Email: apoorvaj@usc.edu

Konstantinos Psounis
Departments of Electrical Engineering and Computer Science
University of Southern California
Los Angeles, CA 90089
Email: kpsounis@usc.edu

***Abstract*— This paper describes a methodology to find the achievable rate region for any static wireless multi-hop network with 802.11 scheduling. To do so, we first characterize the achievable edge-rate region, that is, the set of edge rates that are achievable on the given topology. This requires a careful consideration of the inter-dependence among nearby edges, since neighboring edges collide with and affect the idle time perceived by the edge under study. We use our results to study the optimality of IEEE 802.11 scheduling by comparing the achievable rate region of IEEE 802.11 and optimal scheduling for different scenarios and find that 802.11 is able to achieve more than 80% of the throughput as compared to optimal scheduling for all the scenarios considered. To explain this result, we then characterize the local topologies for which 802.11 scheduling results in a significant drop in throughput as compared to optimal scheduling.**

I. Introduction

A central question in the study of multi-hop networks is the following: Given an arbitrary multi-hop topology and a collection of source-destination pairs, what is the achievable rate region of this arbitrary multi-hop network. Researchers have formulated a multi-commodity flow problem to answer this question [1], [2]. These papers assume optimal TDMA scheduling with different interference models at the MAC layer in their formulations. However, the MAC protocol used in all the multi-hop networks being deployed is IEEE 802.11 [3]–[6]. Characterizing the achievable rate region of an arbitrary multi-hop network with 802.11 scheduling is still an open problem. This characterization will have several applications. For example, it will allow researchers who propose new rate control or routing protocols for multi-hop networks with 802.11 scheduling to compare the performance of their scheme with the optimal value. Further, it will allow the comparison of the achievable rate region of 802.11 scheduling with optimal scheduling to understand where 802.11 stands in terms of optimality.

Setting up a multi-commodity flow formulation for multi-hop networks with 802.11 scheduling runs into the following problem: What is the *achievable edge-rate region* of the given multi-hop topology? The achievable edge-rate region is the region characterizing the set of *edge rates* achievable on the given multi-hop topology. For example, for a wireline network, this region is simply characterized by the constraint that the sum of flow rates at each edge is less than the data rate of the edge. For a multi-hop network with optimal scheduling, this region is characterized using independent sets [1]. Characterizing this region is the main missing step in the characterization of the achievable rate region for multi-hop networks with 802.11 scheduling.

The first main contribution of this work is to characterize the achievable edge-rate region for any given multi-hop topology in a scalable manner. We adopt the following methodology to characterize this region. We first find the expected service time at a particular edge in terms of the collision probability at the receiver and the idle time perceived by the transmitter of that edge. We then derive these collision probabilities and the idle times. Derivation of these probabilities is the harder part in this procedure because their value depends on the edge-rates in the neighborhood around the edge under consideration. Finding the expected service time at each edge allows us to characterize the achievable edge-rate region. We use the characterization of the achievable edge-rate region to characterize the achievable rate region of any given multi-hop network and a collection of source-destination pairs.

The second main contribution of this work is to study the optimality of 802.11 scheduling. We first compare the achievable rate region of 802.11 scheduling and optimal scheduling for three different scenarios. Surprisingly, 802.11 is able to achieve more than 80% of the throughput achieved with optimal scheduling for all the scenarios considered. To understand why we don't see a big drop in the end-to-end rates with 802.11 as compared to optimal scheduling, we also characterize the local topologies for which the achievable edge-rate region will be significantly smaller for 802.11 scheduling.

The outline of this paper is as follows. First, we introduce the network model in Section II. Then, Section III describes a methodology to characterize the achievable edge-rate region of any given multi-hop topology. Section IV uses the achievable edge-rate region to characterize the achievable rate region of the multi-hop network. Section V compares optimal scheduling with IEEE 802.11 for three different scenarios, and then Section VI characterizes the local topologies for which we see a significant drop in local throughput with 802.11 scheduling as compared to optimal scheduling. Finally, Section VII concludes the paper.

II. Network Model

We assume that the static multi-hop topology is given as an input. The connectivity graph of the input topology is denoted by $\mathcal{G} = (V, E)$ where V is the set of all nodes and E is the set of all edges. The interference is assumed to be binary, that is, a transmission emanating from one of the interfering nodes will always cause a collision at the other node, and pairwise, that is, interference happens between node pairs only. Finally, we also assume that a received packet is always decoded successfully in absence of a collision. (To understand the behavior of the MAC layer with interference in a multi-hop network, we have purposely neglected physical layer issues like fading effects, capture effect etc.)

We assume that the set of flows $\mathcal{F}$ is also given as an input. Each flow $f \in \mathcal{F}$ is represented by a source-destination pair. Let $s(f)$ denote the source and $d(f)$ denote the destination for flow f. We assume that the arrival process for each flow f has i.i.d. (independent and identically distributed) inter-arrival times, and has a long-term rate equal to r_f. We also assume independence between the arrival process for different flows. We denote the set of flows flowing through an edge $e \in E$ by $\mathcal{F}_e$ and denote the edge rate (sum of the flow rates at the edge) induced by these flows by λ_e for edge e.

We assume that each node is running IEEE 802.11 with RTS/CTS at the MAC layer. (We assume RTS/CTS because its use is suggested by the 802.11 standard and we do not want to ignore any part of the protocol.) Let W_0 and m denote the initial backoff window and the number of exponential backoff windows respectively. We assume that the basic time unit is equal to one backoff slot time. Let T_{RTS}, T_{CTS}, T_{DATA} and T_{ACK} denote the time taken to transmit one RTS, CTS, DATA and ACK packet respectively. (Note that the DATA packet includes the UDP, IP, MAC and PHY headers along with the payload.) We also assume that all packets are of the same size, so T_{DATA} is a constant. Let T_c denote the time wasted in an RTS collision and let T_s denote the time it takes to complete one packet transmission. Then, $T_c = T_{RTS} + DIFS + \delta$ and $T_s = T_{RTS} + SIFS + \delta + T_{CTS} + SIFS + \delta + T_{DATA} + SIFS + \delta + T_{ACK} + DIFS + \delta$ where δ is the propagation delay and $DIFS$ and $SIFS$ are IEEE 802.11 parameters[1]

III. Characterizing the Achievable Edge-Rate Region

This section characterizes the achievable edge-rate region Λ_E for any multi-hop topology.

A. Expected Service Time for a Particular Edge

This section finds the expected service time of a particular edge (denoted by e) by constructing and solving a Markov chain (MC) for this edge whose states describe the current backoff window, backoff counter, and time since the last successful/unsuccessful RTS/CTS exchange (see next paragraph for details). The transition probabilities of the MC of e depend on the collision probabilities at the receiver of e, which, in turn, depend on the edge-rates at the edges in the neighborhood of e. Hence, these probabilities depend on the exact state of the neighborhood edges. In order to decouple the MCs and reduce the state space, we average these probabilities over all states and work with the average value, following common practice in the analysis of both single hop [8] and multi-hop 802.11 networks [9], [10]. Note that the dependence among neighborhood MCs is captured via these average probabilities. Section III-B describes how to find the value of the collision probabilities, here we just focus on finding the expected service time assuming these probabilities are given.

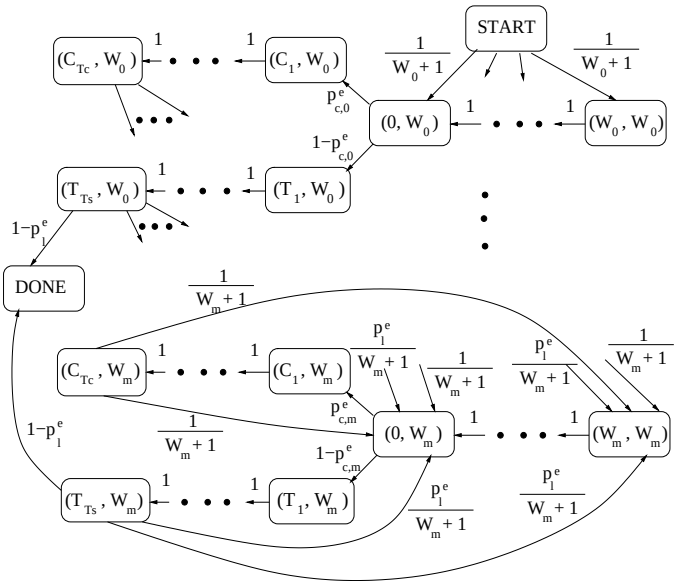

Fig. 1. The Markov chain representing the evolution of a transmitter's state.

The evolution of the 802.11 MAC layer state at the transmitter of edge e after receiving a packet from the network layer is represented by the absorbing MC shown in Figure 1. The MC starts from the state *START* (which represents a packet entering the MAC layer to be scheduled for transmission) and ends in the state *DONE* (which represents the end of a successful packet transmission). The expected service time at e is equal to the expected time it takes for the MC to reach *DONE* from *START*. The state $(j, W_i), 0 \leq j \leq W_i, i = 1, \ldots, 6$, represents the transmitter state where the backoff window is equal to W_i and the backoff counter is equal to j. The backoff counter keeps decrementing till it expires (reaches state $(0, W_i)$) which is then followed by a transmission attempt. The transmitter first attempts an RTS-CTS exchange, which fails with probability $p^e_{c,i}$. (Thus, $p^e_{c,i}$ denotes the probability that the RTS-CTS exchange at edge e is unsuccessful given that the backoff window value at the transmitter of edge e is equal to W_i and either the RTS-CTS or the DATA-ACK exchange was unsuccessful when the backoff window values were $0 \leq j \leq i - 1$.) The states $(C_k, W_i), 1 \leq k \leq T_c$ represent an unsuccessful RTS/CTS exchange C_k time-units before, while the states $(T_k, W_i), 1 \leq k \leq T_s$ represent a

[1]We do not provide a description of IEEE 802.11 protocol. Please refer to [7] for a detailed description of the protocol.

successful RTS-CTS exchange T_k time-units before, followed by the DATA-ACK exchange which fails with probability p_l^e. (Thus, p_l^e denotes the probability that the DATA-ACK exchange is unsuccessful given that the RTS-CTS exchange was successful.) If the DATA-ACK exchange is successful, the MC moves to the state *DONE*. If either the RTS/CTS or the DATA/ACK exchange is unsuccessful, the backoff window is set to $i+1$ if $i < m$, and to m if $i = m$, and the backoff counter is chosen uniformly at random in between 0 and the new backoff window value and the MC jumps to the corresponding state.

Let $E[T_{W_0}]$ denote the additional MC steps required to reach the start of a successful packet transmission given that the packet just exited the START state. Let $E[T^c_{W_i}]$ and $E[T^l_{W_i}]$ for $1 \leq i \leq m$ denote the additional MC steps required to reach the start of a successful packet transmission given that the backoff window just got incremented to W_i due to an unsuccessful RTS-CTS or DATA-ACK exchange respectively. The relationship between these variables is derived using the MC and is summarized in the following equations:

$$\begin{aligned} E[T^c_{W_i}] &= T_c + \tfrac{W_i+1}{2} + p^e_{c,i}E[T^c_{W_{n_i}}] + \left(1-p^e_{c,i}\right)p^e_l E[T^l_{W_{n_i}}] \\ E[T^l_{W_i}] &= T_s + \tfrac{W_i+1}{2} + p^e_{c,i}E[T^c_{W_{n_i}}] + \left(1-p^e_{c,i}\right)p^e_l E[T^l_{W_{n_i}}] \\ E[T_{W_0}] &= \tfrac{W_0+1}{2} + p^e_{c,0}E[T^c_{W_1}] + \left(1-p^e_{c,0}\right)p^e_l E[T^l_{W_1}] \end{aligned} \quad (1)$$

where $n_i = \begin{cases} i+1 & \text{if } 1 \leq i \leq m-1 \\ m & \text{if } i = m \end{cases}$.

Note that this MC does not capture the duration of time the backoff counter may get frozen due to another transmission within the transmitter's neighborhood (due to the virtual carrier sensing mechanism of the 802.11 protocol). To capture this, let p^e_{idle} denote the proportion of time the channel around the transmitter is idle conditioned on the event that the transmitter under consideration is not making a successful transmission. Then, the expected service time at edge e (denoted by $E[S_e]$) is given by the following equation:

$$E[S_e] = T_s + \frac{E[T_{W_0}]}{p^e_{idle}}. \quad (2)$$

To derive the value of the expected service time at a particular edge e using Equations (1) and (2), one has to first find the value of $p^e_{c,i}$, p^e_l and p^e_{idle} for that edge. The value of these variables will depend on the specific topology at hand, and to explicitly show this dependence, from now on we will represent these variables by $p^{e,T}_{c,i}$, $p^{e,T}_l$ and $p^{e,T}_{idle}$ where T represents the topology under study. The next section describes how to find the value of these variables for any edge in a given multi-hop topology.

B. Derivation of Collision and Idle Times

To derive the value of $p^{e,T}_{c,i}$, $p^{e,T}_l$ and $p^{e,T}_{idle}$ for each edge e in topology T, we will first decompose the local topology around the edge into a number of two-edge topologies, and then find these probabilities by appropriately combining the individual probabilities from each two-edge topology. We first define all possible categories of two-edge topologies which can exist in a network [9], [11]. We use the following notation in the definition of these categories: let e_1 and e_2 denote the two edges under consideration and let T_{e_j} and R_{e_j}, $j = 1, 2$, denote the transmitter and the receiver of the two edges. Following is an exhaustive list of different categories of two-edge topologies (Figures 2(a)-2(d) shows an example of each category): (i) Coordinated Stations: A two-edge topology in which T_{e_1} and T_{e_2} can hear each other. (ii) Near Hidden Edges: A two-edge topology in which T_{e_1} and T_{e_2} cannot hear each other, however, there is an edge between T_{e_1} and R_{e_2} as well as T_{e_2} and R_{e_1}. (iii) Asymmetric Topology: A two-edge topology in which T_{e_1} and T_{e_2} as well as T_{e_1} and R_{e_2} cannot hear each other, but T_{e_2} and R_{e_1} are within each other's range. Thus T_{e_2} is aware of the channel state as it can hear the CTS from R_{e_1}, but T_{e_1} is totally unaware of the channel state as it can hear neither the RTS nor the CTS from the transmission on e_2. (iv) Far Hidden Edges: A two-edge topology in which only R_{e_1} and R_{e_2} are within each other's range.

Now we define our notation for this section. Denote by $\mathcal{N}^e$ the set of edges which interfere with the edge under study e. Any edge $e_n \in E \setminus e$ which either forms a coordinated station or asymmetric topology or near hidden edge or far hidden edge with e belongs to this set. We subdivide the edges in $\mathcal{N}^e$ into subsets corresponding to the four two-edge topologies, and the coordinated station topologies and asymmetric topologies are further subdivided into two, giving us the following six sets: (i) $\mathcal{N}^e_1$: edges which form a coordinated station with e and interfere with the receiver of edge e, (ii) $\mathcal{N}^e_2$: edges which form a coordinated station with e and do not interfere with the receiver of edge e, (iii) $\mathcal{N}^e_3$: edges which form a near hidden edge with e, (iv) $\mathcal{N}^e_4$: edges which form an asymmetric topology with e being the edge with an incomplete view of the channel state, (v) $\mathcal{N}^e_5$: edges which form an asymmetric topology with e being the edge which has the complete view of the channel state, and (vi) $\mathcal{N}^e_6$: edges which form a far hidden edge with e.

We only state the value of $p^{e,T}_{c,i}$, $p^{e,T}_l$ and $p^{e,T}_{idle}$ in the following lemmas and skip the proofs for brevity. Please refer to [12] for details. The underlying idea behind all the proofs is to first derive these probabilities for each two-edge topology e is a part of, and then appropriately combine them.

The first lemma states the value of $p^{e,T}_{c,i}$ (the RTS collision probabilities). For coordinated stations and near hidden edges, an RTS collision takes place if the two edges start transmitting at the same time. For near hidden edges, an RTS collision can also take place if a transmitter starts transmitting an RTS while an RTS transmission is ongoing at the other edge. Since the RTS collision probabilities for these two-edge topologies depend on the probability of the backoff counter being equal to zero, these probabilities can be independently combined (as the MC's were assumed to be decoupled). For asymmetric topologies where e has an incomplete view of the channel, and for far hidden edges, the receiver of e will not send back a CTS whenever there is a transmission ongoing at the other edge. Thus, an RTS transmission at e will be successful only if there is no ongoing transmission at any of the edges in $\mathcal{N}^e_4$ and $\mathcal{N}^e_6$. Based on these arguments, we derive the following lemma.

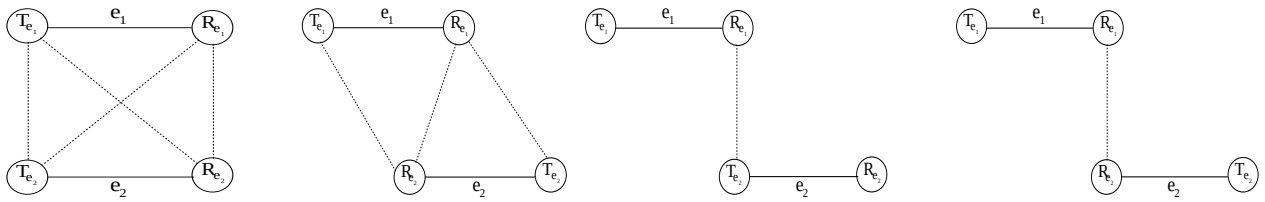

Fig. 2. Different categories of two-edge topologies: (a) Coordinated stations, (b) Near hidden edges, (c) Asymmetric topology, (d) Far hidden edges.

Lemma 3.1: $p_{c,0}^{e,T} = 1 - \left(\left(1 - \prod_{e_n \in \mathcal{N}_1^e} (1 - p_{w0}^{e_n})\right) \times \left(\prod_{e_n \in \mathcal{N}_3^e} \left(1 - 2p_{w0}^{e_n} - \frac{\lambda_{e_n} T_{RTS}}{1 - p_l^{e_n,T}}\right)\right)(1 - P(X))\right)$, and $p_{c,i}^{e,T} = 1 - \left(\left(1 - \left(\left(1 - p_{RTS,0}^{e}\right) p_{c,0}^{e,T} + p_{RTS,0}^{e} p_{r,i}^{e}\right)\right)\right)$ where $p_{w0}^{e_n} = \begin{cases} \frac{2}{W_0^{n}+1} & \text{if } \mathcal{N}_4^{e_n} \cup \mathcal{N}_6^{e_n} = \phi \text{ and } p_l^{e_n,T} \leq p_{cutoff} \\ \frac{2}{W_m^{n}+1} & \text{otherwise} \end{cases}$, $p_{r,i}^{e} = \frac{\sum_{j=0}^{i-1} p^c(j,i) + \sum_{j=0}^{i-1}(1-p(j,i)) p_{c,0}^{e,T}}{\prod_{u=1}^{i-1}\left(p_{c,u}^{e,T} + \left(1 - p_{c,u}^{e,T}\right) p_l^{e,T}\right)}$, $p_{RTS,0}^{e} = \frac{P(X)}{p_{c,0}^{e,T} + \left(1 - p_{c,0}^{e,T}\right) p_l^{e,T}}$, and $P(X) = P\left(\cup_{e_n \in \mathcal{N}_4^e \cup \mathcal{N}_6^e} X_{e_n}\right)$, where X_{e_n} is the event that a transmission is ongoing at edge e_n.

Please refer to [12] for the description and values of $p(j,i), p^c(j,i)$ and p_{cutoff}. Next, we state the value of $P(X)$ in the following lemma.

Lemma 3.2: $P\left(\cup_{e_n \in N} X_{e_n}\right) = \sum_{e_i \in N} P(X_{e_i}) - \sum_{e_i, e_j \in N} P(X_{e_i} \cap X_{e_j}) + \ldots + (-1)^{|N|-1} P(\cap_{e_i \in N} X_{e_i})$, where $N = \mathcal{N}_4^{e_n} \cup \mathcal{N}_6^{e_n}$, $P(X_{e_i}) = \frac{\lambda_{e_i} T_s}{1 - p_l^{e_i,T}}$ and $P(\cap_{e_i \in N_s} X_{e_i})$ for $N_s \subset N$ is equal to 0 if any two edges in N_s interfere with each other , otherwise it is equal to $\left(\prod_{e_i \in N_s} \frac{\lambda_{e_i} T_s}{1 - p_l^{e_i,T}}\right) \frac{1}{\left(1 - \sum_{e_k \in S_{N_s}} \frac{\lambda_{e_k} T_s}{1 - p_l^{e_k,T}}\right)^{|N_s|-1}}$ where S_{N_s} denotes the set of edges in E which interfere with all the edges in N_s.

Next we derive the value of $p_l^{e,T}$ (DATA collision probability). DATA collisions can happen only for asymmetric topologies where e does not have a complete view of the channel state. If the receiver of e starts transmitting the CTS and the transmitter of the other edge starts transmitting an RTS at the same time, then both these packets will be successfully received and will result in a DATA collision at e. Based on this intuition, we derive the value of $p_l^{e,T}$ in the following lemma.

Lemma 3.3: $p_l^{e,T} = 1 - \left(\prod_{e_n \in \mathcal{N}_4^e} (1 - \lambda_{e_n} E[S_{e_n}] p_{w0}^{e_n})\right)$.

Finally, we derive the value of $p_{idle}^{e,T}$ based on the observation that the backoff counter at e will be frozen whenever there is a transmission ongoing at any of the edges in $\mathcal{N}_1^e, \mathcal{N}_2^e, \mathcal{N}_3^e$ and $\mathcal{N}_5^e$.

Lemma 3.4: Assuming the time taken to transmit one RTS, T_{RTS}, is significantly smaller than the time taken to complete one transmission, T_s, $p_{idle}^{e,T} = \frac{1 - P\left(\cup_{e_n \in \mathcal{N}_1^e \cup \mathcal{N}_2^e \cup \mathcal{N}_3^e \cup \mathcal{N}_5^e} X_{e_n}\right) - \lambda_e T_s}{1 - \lambda_e T_s}$.

Equations (1) and (2) along with the expressions derived in this section enable the derivation of the expected service time at any edge in any multi-hop topology. Thus, these equations along with the constraints $\sum_{e \in O_v} \lambda_e E[S_e] \leq 1, \forall v \in V$, (where O_v represents the set of outgoing edges from a node v) characterize the achievable rate region Λ_E. (We sum over all outgoing edges from a node because the network queue for all outgoing edges at a node is the same.)

IV. Characterizing the Achievable Flow Rate Region

The achievable flow rate region of a given multi-hop network and a collection of source-destination pairs is characterized by the set of the following constraints:

$$\begin{aligned} r_f &\geq 0 && \forall f \in \mathcal{F} \\ \lambda_e &= \sum_{f \in \mathcal{F}} r_f^e && \forall e \in E \\ g(f) + \sum_{e \in I_v} r_f^e &= \sum_{e \in O_v} r_f^e && \forall f \in \mathcal{F}, \forall v \in V \\ \vec{\lambda}_e &\in \Lambda_E \end{aligned}$$

where r_f^e denotes the flow rate of flow f flowing through edge e, $g(f) = \begin{cases} r_f & \text{if } v = s(f) \\ -r_f & \text{if } v = d(f) \\ 0 & \text{otherwise} \end{cases}$ and I_v and O_v denote the set of incoming edges into and outgoing edges from the node v respectively. The first constraint ensures non-negativity of flow rates, the second constraint expresses edge rates in terms of flow rates and the third constraint is the standard flow conservation constraint. The final constraint says that the vector of edge rates $\vec{\lambda}_e$ induced at the edges should lie within the achievable edge-rate region.

V. IEEE 802.11 vs Optimal Scheduling: End-to-End Throughput

In this section, we compare the achievable rate region for IEEE 802.11 with the capacity region for optimal scheduling for three different scenarios. We use the methodology proposed in [1] to find the capacity region for optimal scheduling and the methodology introduced in the previous two sections to find the achievable rate region with 802.11 scheduling. For a fairer comparison, we also incorporate the overhead due to UDP, IP, MAC and PHY headers and link layer ACKs (assuming that the MAC and PHY header sizes and the ACK packet size for optimal scheduling are the same as 802.11) in the derivation of the capacity region for optimal scheduling. However, we do not incorporate the overhead required in constructing and distributing the optimal schedule.

Packet Payload	1024 bytes
MAC Header	34 bytes
PHY Header	16 bytes
ACK	14 bytes + PHY header
RTS	20 bytes + PHY header
CTS	14 bytes + PHY header
Channel Bit Rate	1 Mbps
Propagation Delay	1 μs
Slot Time	20 μs
SIFS	10 μs
DIFS	50 μs
W_0	31
m	6

TABLE I

SYSTEM PARAMETERS USED TO OBTAIN NUMERICAL RESULTS.

To obtain numerical results, most of the 802.11 protocol parameters are set to the default values of 802.11(b) and are summarized in Table I. The channel bandwidth is set to the lowest MAC data rate for 802.11(b) which is equal to 1 Mbps, and the packet size is assumed to be 1024 bytes.

A. Scenario 1: Flow in the Middle

Figure 3(a) shows the Flow in the Middle topology. Flows 1 and 3 do not interfere with each other, but both of them interfere with flow 2.[2] Different papers have used this topology or a similar topology to demonstrate the unfairness of the 802.11 protocol towards flow 2 (which is competing with two flows) under backlogged conditions [13] or with TCP [14].

Since flows 1 and 3 are symmetric, we assume that $r_{f_1} = r_{f_3}$ and plot the achievable rate region for 802.11 and capacity region for optimal scheduling for this equal rate against r_{f_2} in Figure 3(b). (The routing is assumed to be fixed for this scenario.) We make the following observations from this figure: (i) IEEE 802.11 is always able to achieve more than 80% of the throughput as compared to optimal scheduling. (ii) The max-min fair flow rate allocation for this topology with IEEE 802.11 is to assign 0.186 Mbps to all the three flows, while optimal scheduling assigns 0.223 Mbps to all the three flows. (iii) As expected, the maximum throughput for this system is achieved when flow 2 is switched off, and is equal to 0.828 Mbps for 802.11 (as compared to 0.558 Mbps achieved with max-min fair flow rate allocation).

B. Scenario 2: Multi-path Routing Can Increase Throughput

In the next two scenarios, we study multi-path routing with 802.11 scheduling in multi-hop networks. Figure 3(c) shows the topology considered in this scenario. Consider a flow with node 1 as the source and node 8 as the destination. There are two possible routes to route packets from 1 to 8: $1 \rightarrow 2 \rightarrow 3 \rightarrow 4 \rightarrow 8$ and $1 \rightarrow 5 \rightarrow 6 \rightarrow 7 \rightarrow 8$. With optimal scheduling, one can achieve a throughput of 0.445 Mbps by routing half the packets along the first route and the other half along the second route. With IEEE 802.11 scheduling, throughput is again maximized by sending half the packets along the first route and the other half along the second route. This multi-path routing scheme achieves a throughput of 0.392 Mbps. (Single-path routing scheme achieves a maximum of 0.262 Mbps by routing along one of the either two paths.) We made the following observations by studying this scenario: (i) Even though multi-path routing increases the number of collisions at each edge for 802.11 scheduling, it still increases the throughput. (ii) 802.11 is able to achieve 88% of the throughput achieved with optimal scheduling. (iii) The queue at node 1 turned out to be the most congested because it contains packets for two edges and head of line blocking in this queue decreases the overall throughput. Maintaining a separate network queue for each edge increases the throughput of this scenario to 0.4 Mbps.

[2]We say that two flows interfere with each other if any two edges over which they are routed interfere with each other

C. Scenario 3: Multi-path Routing is Not Always Optimal

We consider the topology of Figure 3(c) again. Now, there are two flows in the network, one flowing from node 1 to node 8 (flow 1) and another flowing from node 8 to node 1 (flow 2). There are two possible routes for both the flows. We plot the achievable flow rate region (r_{f_1} vs r_{f_2}) with 802.11 scheduling and the capacity region achieved with optimal scheduling in Figure 3(d). We make the following observations from this figure: (i) With optimal scheduling, one achieves a max-min fair rate allocation of 0.223 Mbps per flow with both single-path and multi-path routing. However with 802.11 scheduling, the max-min fair rate allocation of 0.204 Mbps per flow is achieved only with single-path routing. (Max-min fair rate allocation with multi-path routing is equal to 0.198 Mbps per flow.) (ii) 802.11 is able to achieve more than 80% of the throughput as compared to optimal scheduling.

D. Summary

Now we summarize the results of this section. (i) IEEE 802.11 is able to achieve more than 80% of the throughput as compared to optimal scheduling for all the three scenarios considered. Note that we cannot generalize the conclusions about the optimality of 802.11 from these three scenarios. So, we investigate this question further in the next section. (ii) Multi-path routing creates more collisions at each edge, hence it may or may not be better than single-path routing when 802.11 scheduling is used. (iii) Fairness without a significant loss in throughput with 802.11 scheduling can always be achieved with suitable rate control.

VI. IEEE 802.11 VS OPTIMAL SCHEDULING: LOCAL THROUGHPUT

To understand why we don't see a big drop in the end-to-end rates with 802.11 as compared to optimal scheduling, in this section we characterize the local topologies for which the achievable edge-rate region will be significantly smaller for IEEE 802.11 scheduling than optimal scheduling. (By local topologies, we imply that we will compare only the local edge rates and not the end-to-end flow rates.)

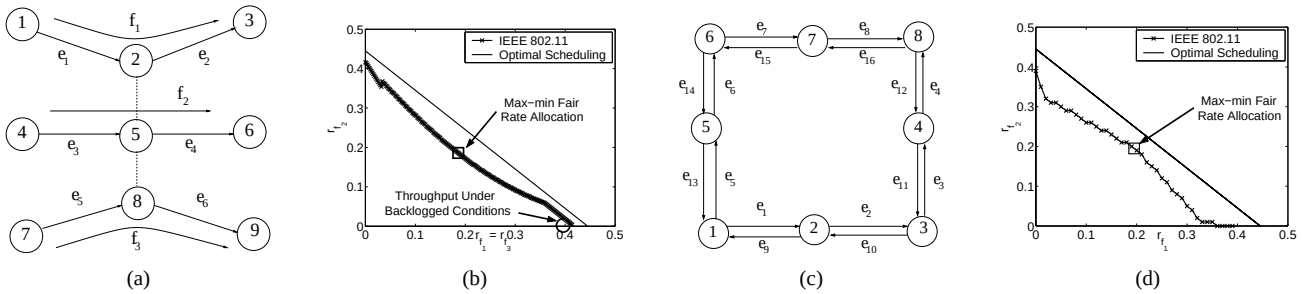

Fig. 3. (a) The Flow in the Middle topology. (b) Capacity Region for the Flow in the Middle Topology. (c) Topology used in scenarios 2 and 3. (d) Capacity Region for scenario 3.

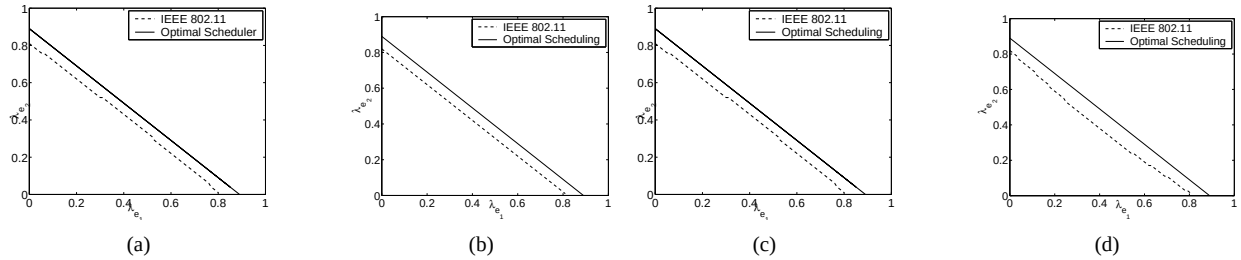

Fig. 4. Achievable edge-rate region for IEEE 802.11 and optimal scheduling for the different categories of two-edge topologies: (a) Coordinated Stations, (b) Near Hidden Edges, (c) Asymmetric Topology, and (d) Far Hidden Edges.

We first compare the achievable edge-rate regions for the four categories of two-edge topologies in Figures 4(a)-4(d). Amongst these four categories, the asymmetric topology has the smallest achievable rate region (largest drop in throughput).

Next we look at three-edge topologies. The three edges are denoted by e_1, e_2 and e_3, and without loss of generality, let e_1 be the edge under consideration. The local topology is defined by which two-edge topology describes the relationship between edges e_1 and e_2 and between e_1 and e_3 and whether e_2 and e_3 interfere with each other or not (as the combined effect of e_2 and e_3 on e_1 does not depend on which of the four two-edge topologies they belong to, it just depends on whether they interfere with each other or not). Finally, for each topology, to compare 802.11 scheduling with optimal scheduling, we will state the loss in throughput with 802.11 for the best equal rate allocation.

The first scenario we consider is the one shown in Figure 5(a). e_1 interferes asymmetrically with both e_2 and e_3, while e_2 and e_3 do not interfere with each other and can be scheduled simultaneously. However, 802.11 will schedule e_2 and e_3 independently and not simultaneously, which decreases the proportion of time neither of them is transmitting, and hence increases the probability of collisions at e_1. As a result, 802.11 will perform worse than the optimal scheduler. In particular, from the achievable rate region we derive that its best equal rate is less than 70% of the rate achieved by the optimal scheduler. If the relationship between e_1 and e_2, and e_1 and e_3 is far hidden edges, then 802.11 is able to achieve 83% of the throughput achieved by optimal scheduling. Finally, if the relationship between e_1 and e_2, and e_1 and e_3 is either coordinated stations or near hidden edges, 802.11 suffers from very few collisions and is able to perform closer to the optimal. In particular, in these cases it achieves more than 85% of the optimal throughput.

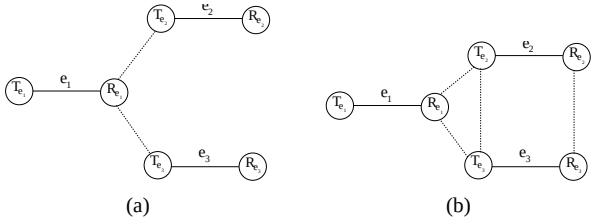

Fig. 5. (a) First topology used to compare local edge rates achieved with 802.11 as compare to optimal scheduling. (b) Second topology used to compare local edge rates achieved with 802.11 as compare to optimal scheduling.

The next scenario we consider is the one shown in Figure 5(b). e_1 interferes asymmetrically with both e_2 and e_3 for the channel, while e_2 and e_3 interfere with each other. Neither optimal scheduling nor 802.11 will schedule e_2 and e_3 simultaneously, and 802.11 achieves more than 80% of the optimal throughput. If the relationship between e_1 and e_2, and e_1 and e_3 is either coordinated station or near hidden edges or far hidden edges, again 802.11 is able to achieve more than 80% of the throughput achieved by optimal scheduling. Thus, only one three-edge topology suffers from a significant loss in throughput with 802.11 scheduling as compared to optimal scheduling.

Finally, if we add another edge e_4 to the three-edge topologies, if e_1 interferes asymmetrically with e_2, e_3, e_4 and e_2, e_3 and e_4 do not interfere with each other, then 802.11 is able to achieve only 62% of the optimal throughput, while for the

other four-edge topologies, 802.11 achieves more than 80% of the optimal throughput. Hence, quite surprisingly, 802.11 achieves more than 80% of the rates achieved by optimal scheduling in all but one type of local topology. Specifically, it performs bad only if there exists an edge which interferes asymmetrically with multiple links which do not interfere with each other and can be scheduled independently. This suggests that for multi-hop networks with 802.11 scheduling, routing protocols should avoid routing through such local topologies and topology control protocols should focus on weeding out the existence of such local topologies.

As a final note, we would like to point out that our results refer to the best achievable rates without specifying the protocols used to achieve it, and they are by no means contradictory to the well-known fact that TCP over 802.11 may have very bad performance [14], [15].

VII. Conclusions

This paper characterizes the achievable rate region of an arbitrary multi-hop wireless network with 802.11 scheduling by deriving a methodology to characterize the achievable edge-rate region. We then use this characterization to study the optimality of IEEE 802.11 by comparing the achievable rate region of 802.11 and optimal scheduling for different scenarios. We find that 802.11 is able to achieve more than 80% of the throughput achieved by optimal scheduling for all the scenarios considered. To understand this result, we characterize the local topologies for which 802.11 results in a significant loss in throughput and find only one such type of local topology.

References

[1] K. Jain, J. Padhye, V. Padmanabhan, and L. Qiu, "Impact of interference on multi-hop wireless network performance," in *Proceedings of ACM MOBICOM*, 2003.

[2] V. Kumar, M. M.V, S. Parthasarathy, and A. Srinivasan, "Algorithmic aspects of capacity in wireless networks," in *Proc. ACM Sigmetrics*, 2005.

[3] J. Bicket, D. Aguayo, S. Biswas, and R. Morris, "Architecture and evaluation of an unplanned 802.11b mesh network," in *Proceedings of ACM MOBICOM*, 2005.

[4] Y. Sun, I. Sheriff, E. Belding-Royer, and K. Almeroth, "An experimental study of multimedia traffic performance in mesh networks," in *Proceedings of WitMeMo*, 2005.

[5] J. Eriksson, S. Agarwal, P. Bahl, and J. Padhye, "Feasibility study of mesh networks for all-wireless offices," in *Proceedings of ACM MOBISYS*, 2006.

[6] J. Camp, J. Robinson, C. Steger, and E. Knightly, "Measurement driven deployment of a two-tier urban mesh access network," in *Proceedings of ACM MOBISYS*, 2006.

[7] "Draft supplement to part 11, wireless medium access control (MAC) and physical layer (PHY) specifications: medium access control (MAC) quality of service (QoS) enhancements," *IEEE Std. 802.11e/D4.0*, nov 2002.

[8] G. Bianchi, "Performance analysis of the ieee 802.11 distributed coordination function," *IEEE Journal on Selected Areas in Communications*, vol. 18, pp. 535–547, Mar. 2000.

[9] M. Garetto, T. Salonidis, and E. Knightly, "Modeling per-flow throughput and capturing starvation in csma multi-hop wireless networks," in *Proceedings of ACM INFOCOM*, 2006.

[10] K. Medepalli and F. A. Tobagi, "Towards performance modeling of ieee 802.11 based wireless networks: A unified framework and its applications," in *Proceedings of ACM INFOCOM*, 2006.

[11] M. Garetto, J. Shi, and E. Knightly, "Modeling media access in embedded two-flow topologies of multi-hop wireless networks," in *Proceedings of ACM MOBIHOC*, 2005.

[12] A. Jindal and K. Psounis, "Characterizing the achievable rate region for multi-hop wireless networks with IEEE 802.11 scheduling (Available on Request)," USC, Tech. Rep. CENG-2007-12, 2007.

[13] X. Wang and K. Kar, "Throughput modeling and fairness issues in CSMA/CA based ad-hoc networks," in *Proceedings of IEEE INFOCOM*, 2005.

[14] K. Xu, M. Gerla, L. Qi, and Y. Shu, "TCP unfairness in ad-hoc wireless networks and neighborhood RED solution," in *Proceedings of ACM MOBICOM*, 2003.

[15] K. Nahm, A. Helmy, and C. J. Kuo, "TCP over multihop 802.11 networks: issues and performance enhancements," in *Proceedings of ACM MOBIHOC*, 2005.